


Metal-free Inorganic Ligands for Colloidal Nanocrystals: S^{2-} , HS^- , Se^{2-} , HSe^- , Te^{2-} , HTe^- , TeS_3^{2-} , OH^- , and NH_2^- as Surface Ligands

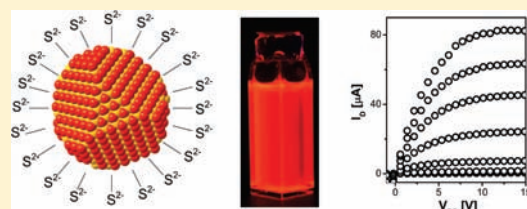
Angshuman Nag,[†] Maksym V. Kovalenko,[†] Jong-Soo Lee,[†] Wenyong Liu,[†] Boris Spokoyny,[†] and Dmitri V. Talapin^{*,†,‡}

[†]Department of Chemistry and James Frank Institute, University of Chicago, Illinois 60637, United States

[‡]Center for Nanoscale Materials, Argonne National Laboratory, Argonne, Illinois 60439, United States

 Supporting Information

ABSTRACT: All-inorganic colloidal nanocrystals were synthesized by replacing organic capping ligands on chemically synthesized nanocrystals with metal-free inorganic ions such as S^{2-} , HS^- , Se^{2-} , HSe^- , Te^{2-} , HTe^- , TeS_3^{2-} , OH^- and NH_2^- . These simple ligands adhered to the NC surface and provided colloidal stability in polar solvents. The versatility of such ligand exchange has been demonstrated for various semiconductor and metal nanocrystals of different size and shape. We showed that the key aspects of Pearson's hard and soft acids and bases (HSAB) principle, originally developed for metal coordination compounds, can be applied to the bonding of molecular species to the nanocrystal surface. The use of small inorganic ligands instead of traditional ligands with long hydrocarbon tails facilitated the charge transport between individual nanocrystals and opened up interesting opportunities for device integration of colloidal nanostructures.



1. INTRODUCTION

During past years, significant attention has been paid to the applications of colloidal nanocrystals (NCs) in electronic and optoelectronic devices.^{1–4} These require facile transport of charge carriers through NCs. The efficiency of moving charges in and out of NCs strongly depends on the NC environment.^{5–8} The surface of NCs prepared by traditional colloidal techniques is capped with a layer of ligands with long hydrocarbon tails which introduce insulating layers around each NC.⁸ As a result, the benefits of quantum-confined materials are often outweighed by inefficient injection (e.g., in LEDs) or extraction (in solar cells and photodetectors) of electrons and holes.

We recently introduced the concept of inorganic molecular metal chalcogenide (MCC) ligands that provided colloidal stabilization without blocking the interparticle charge transport.^{9–11} The MCC ligands contain main group or transition metals bound to the NC surface through chalcogenide bridges. The presence of foreign metal ions in a close proximity to the NC surface could in some cases affect the chemical and physical properties. For example, metal ions from MCC ligands can participate in redox processes, as in the case of $Sn_2S_6^{4-}$ ligands that can switch between Sn^{IV} and Sn^{II} oxidation states. These potential complications could be avoided by introducing metal-free inorganic ligands.

In this work, we explored new surface chemistries for all-inorganic colloidal NCs and introduced metal-free inorganic ligands, such as chalcogenides and hydrochalcogenides (S^{2-} , HS^- , Se^{2-} , HSe^- , Te^{2-} , and HTe^-), mixed chalcogenides (TeS_3^{2-}), as well as OH^- and NH_2^- . These inorganic ions bind to the surface of semiconductor and metal NCs and provide electrostatic stabilization for colloidal dispersions in polar solvents. These ligands are probably

the simplest, cheapest, and smallest ones for colloidal NCs and they can find broad use in NC-based devices. In fact, similar concept of colloidal stabilization was first reported more than a century ago when I^- ions were employed to stabilize AgI colloids.^{12,13} We develop that “old” chemistry further by showing that inorganic anions can displace the organic ligands from the surface of various technologically important sub-10 nm colloidal NCs.

2. EXPERIMENTAL SECTION

2.1. Nanocrystal Synthesis. Zinc blende phase CdSe NCs capped with oleic acid and oleylamine were prepared following Cao et al.¹⁴ Wurtzite phase CdSe NCs capped with *n*-octadecylphosphonic acid (ODPA) were prepared from CdO and *n*-trioctylphosphine selenide (TOPSe) following Manna et al.¹⁵ Large, 12 nm CdSe NCs capped with *n*-tetradecylphosphonic acid (TDPA) were synthesized using Cd(CH_3)₂ and TOPSe as precursors.¹⁶ We also used CdSe and CdSe/ZnS core/shell NCs capped with proprietary ligands obtained from Evident Technologies, Inc. (Troy, NY). These CdSe/ZnS core/shell NCs showed photoluminescence quantum efficiency about 65%.

To synthesize InP NCs, InCl₃ solution (1.036 g of InCl₃ in 3.44 mL of TOP), 0.75 g of P(SiMe₃)₃, 7.4 g of TOP, and 0.9 g of TOPO were mixed at room temperature. The mixture was heated to 270 °C for 2 days, and cooled down to room temperature.^{17,18} Postsynthesis size selective precipitation was carried out using toluene and ethanol as solvent and nonsolvent, respectively.

Received: April 10, 2011

Published: June 17, 2011

InAs NCs with TOP as capping ligands were prepared from InCl_3 and $\text{As}[\text{Si}(\text{CH}_3)_3]_3$.^{19,20}

Au NCs were synthesized following Stucky et al.;²¹ 0.25 mmol AuPPh₃Cl was mixed with 0.125 mL of dodecanethiol in 20 mL of benzene forming a clear solution. Then, 2.5 mmol *tert*-butylamine-borane complex was added to the above mixture followed by stirring at 80 °C.

ZnSe NCs were prepared following ref 22 with some modifications. Seven milliliters of oleylamine was degassed at 125 °C under vacuum for 30 min and then heated to 325 °C under N₂ flow. The solution containing 0.5 M Zn and Se precursors was prepared by co-dissolution of diethylzinc and Se in TOP at room temperature. Two milliliters of the precursors solution was added to degassed oleylamine at 325 °C. One milliliter of additional precursors solution was added to the reaction mixture after 1 h, followed by two successive injections of 1.5 mL of precursors solution after 2.5 and 4 h. The reaction was continued for 1 h after the final injection of the precursors and then cooled to room temperature. The NCs were washed by precipitation with ethanol and redispersed in hexane. The washing procedure was repeated three times.

CdS nanorods were prepared by slightly modified procedure described in ref 23; 0.207 g of CdO, 1.08 g of *n*-ODPA, 0.015 g of *n*-propylphosphonic acid, and 3.35 g of TOPO were heated at 120 °C under vacuum for 1 h, followed by heating the mixture to 280 °C under N₂ until the formation of a clear solution. The mixture was degassed at 120 °C for 2 h before it was heated to 300 °C under N₂. Two grams of TOP was injected into the mixture at 300 °C and temperature was immediately set to 320 °C. Then, 1.30 g of *n*-trioctylphosphine sulfide (TOPS) was injected at 320 °C and heating was continued for 2 h. The reaction mixture was cooled to room temperature, washed twice with toluene/acetone, and redispersed in toluene.

In₂O₃ NCs were prepared using the recipe of Seo et al.²⁴ by heating a slurry of In(OAc)₃ and oleylamine at 250 °C.

CdTe NCs were synthesized similar to the recipe published in ref 25.

PbS NCs capped with oleic acid were synthesized according to the protocol developed by Hines et al.²⁶

2.2. Synthesis of Inorganic Ligands. Alkali metal sulfides, hydrogen sulfide, hydroxides, and amide ligands were purchased from Aldrich and Strem and used as received.

K₂Se was synthesized by the reaction of K (25.6 mmol) with Se (12.8 mmol) in about 50 mL of liquid ammonia.^{27,28} Special care was taken to make sure that the chemicals and reaction environment were air and moisture free. A mixture of dry ice and acetone was used to liquefy NH₃ gas. Gray-white K₂Se powder was stored inside a glovebox. In air, K₂Se turned red because of the formation of polyselenides. K₂Te was prepared in the same way as K₂Se; 7.6 mmol of K and 3.8 mmol of Te were used.

The 0.05 M solutions of KHSe and KHTe in formamide (FA) were prepared by titrating 25 mL of 0.05 M KOH solution with H₂Se (or H₂Te) gas generated by the reaction of Al₂Se₃ (or Al₂Te₃) with 10% H₂SO₄. A 1.7-fold molar excess of H₂Se (or H₂Te) was used. Rigorous N₂ environment was maintained while handling the KHSe and KHTe solutions.

(NH₄)₂TeS₃ was synthesized using a modified literature method of Gerl et al.²⁹ 2TeO₂·HNO₃ was prepared by dissolving 5 g of Te (pellets, Aldrich) in 35 mL of HNO₃ (65%, aqueous) diluted with 50 mL of H₂O. The solution was boiled in an open beaker until volume decreased to about 30 mL. Upon cooling, 2TeO₂·HNO₃ was precipitated as a white solid that was separated by filtering, rinsed with deionized water and dried. To prepare (NH₄)₂TeS₃, 2 g of 2TeO₂·HNO₃ was mixed with 40 mL of aqueous ammonia solution (~30% NH₃, Aldrich). Solution was first purged with N₂ for 5 min, then with H₂S until all telluronitrate dissolved forming a yellow solution, characteristic for TeS₃²⁻ ions. Solvents and (NH₄)₂S were removed by vacuum evaporation. The solid was redispersed in 36 mL of H₂O, 4 mL of NH₄OH, and 0.1 mL of N₂H₄ (used as a stabilizer against oxidative decomposition) forming a clear

yellow solution of TeS₃²⁻ ions (with small amounts of Te₂S₅²⁻ as confirmed by ESI-MS) at a concentration of about 0.25M.

2.3. Ligand Exchange. **2.3.1. Ligand Exchange with Chalcogenide (S²⁻, Se²⁻, Te²⁻) and Hydrochalcogenide (HS⁻, HSe⁻, HTe⁻) Ions.** The ligand exchange process was typically carried out under inert atmosphere. Colloidal dispersions of different NCs with organic ligands were prepared in nonpolar solvents like toluene or hexane, while solutions of inorganic ligands were prepared in polar formamide (FA) immiscible with toluene and hexane. For a typical ligand exchange using S²⁻ ions, 1 mL of CdSe NC solution (~2 mg/mL) was mixed with 1 mL of K₂S solution (5 mg/mL). The mixture was stirred for about 10 min leading to a complete phase transfer of CdSe NCs from toluene to the FA phase. The phase transfer can be easily monitored by the color change of toluene (red to colorless) and FA (colorless to red) phases. The FA phase was separated out followed by triple washing with toluene to remove any remaining nonpolar organic species. The washed FA phase was then filtered through a 0.2 μm PTFE filter and ~1 mL of acetonitrile was added to precipitate out the NCs. The precipitate was redispersed in FA and used for further studies. The NC dispersion in FA was stable for months. Ligand exchange with Se²⁻, Te²⁻, HS⁻, HSe⁻, and HTe⁻ ligands was carried out in a similar manner. In some cases, the ligand exchange took longer time, up to several hours.

The exchange of organic ligands with S²⁻ and SH⁻ can be carried out in air as well. Moreover, one can use concentrated aqueous solutions of (NH₄)₂S, K₂S, and Na₂S as S²⁻ source to carry out the ligand exchange. As an example, 10 μL of (NH₄)₂S solution (Aldrich, 40–48 wt % in water) was added to 1 mL of FA and mixed with NC dispersion in toluene or hexane. The rest of the ligand exchange procedure was similar to the above protocol. When handled in air, the solutions of S²⁻-capped NCs preserve their colloidal stability for only several days. Resulting precipitates could be easily redispersed after addition of ~5 μL (NH₄)₂S solution; the dispersions stabilized with additional S²⁻ remained stable for several weeks in air. Similar to water and FA, the ligand exchange can be carried out in DMSO.

2.3.2. Ligand Exchange with TeS₃²⁻. The mixed chalcogenide Te–S species are stable in basic solutions (we typically added NH₄OH) and are highly susceptible to oxidation. All ligand-exchange reactions were carried out in a glovebox. In a typical ligand exchange for CdTe NCs, 0.4 mL of CdTe NCs capped with oleic acid in toluene (~25 mg/mL) was mixed with 3 mL of FA, 3 mL of toluene, and 0.4 mL of ~0.25 M (NH₄)₂TeS₃ solution. Upon stirring for 2–10 h, CdTe NCs quantitatively transferred into FA phase. NC solution was rinsed 3 times with toluene and mixed with 3–6 mL of acetonitrile. NCs were isolated by centrifuging and redispersed in FA.

2.3.3. Ligand Exchange with OH⁻. A stock solution of KOH was prepared by dissolving 135 mg of KOH in 0.4 mL of FA. For a typical ligand exchange reaction, ~2 mg of 5.5 nm CdSe NCs was dispersed in 1 mL of toluene. One milliliter of FA was added to the NC solution followed by the addition of 20 μL of KOH solution and stirred for about 10 min. Red colored FA phase was separated out, washed three times with toluene, and passed through a 0.2 μm PTFE filter. Acetonitrile was added to precipitate the NCs, followed by centrifugation and redispersion of NCs in FA. The process was carried out under inert atmosphere.

2.3.4. Ligand Exchange with NH₂⁻. A total of 0.05 g of NaNH₂ was dissolved in 0.5 mL of FA to prepare a stock solution. Then, 0.1 mL of the NaNH₂ stock solution was diluted to 1 mL by adding FA and the resulting solution was added to 1.5 mg of CdSe NCs dispersed in 1 mL of toluene. The mixture was stirred for about 10 min. The NCs were separated out to the FA phase, washed, precipitated, centrifuged, and redispersed in FA under inert atmosphere.

2.3.5. Treatment with HBF₄ and HPF₆. A total of 1.5 mg of CdSe NCs was dispersed in 1 mL of toluene followed by the addition of a solution of HBF₄ (prepared by mixing 25 μL of 50 wt % aqueous HBF₄ with 1 mL of FA). NCs completely transferred to the FA phase within 5 min. The

colorless toluene phase was discarded followed by the addition of pure toluene to wash out any remaining nonpolar organics. The washing was repeated 3–4 times in about 30 min and finally the NCs dispersed in FA were passed through a 0.2 μm PTFE filter. HPF₆ treatment was carried out in similar manner. All these steps were carried out under the nitrogen environment inside a glovebox, and the FA dispersion of CdSe NCs obtained after the ligand exchange was found to be stable for a few days, after which the NCs precipitate out of the solution.

2.4. Characterization. UV–vis absorption spectra of NC dispersions were recorded using a Cary 5000 UV–vis-NIR spectrophotometer. Photoluminescence (PL) spectra were collected using a FluoroMax-4 spectrofluorometer (HORIBA Jobin Yvon). PL quantum efficiency of the NC dispersions were measured using Rhodamine 6G (QE = 95%) as a reference dye dissolved in ethanol. Fourier-transform infrared (FTIR) spectra were acquired in the transmission mode using a Nicolet Nexus-670 FTIR spectrometer. Samples for FTIR measurements were prepared by drop casting concentrated NC dispersions on KBr crystal substrates (International Crystal Laboratories) followed by drying at 90 °C under vacuum. Transmittance of different NC samples was normalized by the weight of NCs per unit area of the deposited film, assuming a uniform film thickness across the KBr substrate. Transmission Electron Microscopy (TEM) data were obtained using a FEI Tecnai F30 microscope operated at 300 kV. Dynamic light scattering (DLS) and ζ -potential data were obtained using a Zetasizer Nano-ZS (Malvern Instruments, U.K.). ζ -potential was calculated from the electrophoretic mobility using Henry's equation in the Smoluchowski limit.³⁰ Electrospray ionization mass spectrometry (ESI-MS) was performed using Agilent 1100 LC/MSD mass-spectrometer. The peak assignments were based on the comparison of experimental mass-spectra with calculated isotope patterns.

2.5. Charge Transport Studies. **2.5.1. Device Fabrication.** All fabrication steps were carried out under dry nitrogen atmosphere. Highly p-doped Si wafers (Silicon Quest, Inc.) with a 100 nm thick layer of thermally grown SiO₂ gate oxide were used as a substrate. The oxide layer on the back side of the wafers was etched using 1% HF aqueous solution, followed by careful rinsing with high purity deionized water. The substrates were cleaned with acetone, isopropyl alcohol, and ethanol, followed by drying in a flow of N₂ gas. SiO₂ surface was hydrophilized by oxygen plasma or piranha (H₂SO₄/H₂O₂) treatments immediately prior to NC deposition. The substrates were treated by oxygen plasma (~80W) for 10–15 min. Piranha treatment was usually carried out at 120 °C for 10 min followed by multiple washings with high purity deionized water. Piranha solution was prepared by adding concentrated sulfuric acid to 30% H₂O₂ solution (2:3 volume ratio).

The NC films for electrical measurements were prepared by depositing thin 20–40 nm films by spin-coating (spread: 600 rpm, 6 s; spin: 2000 rpm, 30 s) from FA solutions at elevated temperatures (80 °C) using a 500 W infrared lamp placed above the substrate. After deposition, the NC films were dried at 80 °C for 30 min, followed by annealing at 200–250 °C for 30 min using a hot plate with calibrated temperature controller. Such heating of NC films removes solvents and remaining volatile ligands. The NC film thickness was measured using AFM or high resolution SEM of device cross sections. The top source and drain electrodes were thermally evaporated at 1.0–2.5 Å/s rate up to ~1000 Å total thickness using a metal evaporator located inside nitrogen-filled glovebox. After deposition of Al electrodes, the devices were post annealed at 80 °C for 30 min to improve the contacts.

2.5.2. Electrical Measurements. All electrical measurements were performed using Agilent B1500A semiconductor parameter analyzer. The source electrode was grounded for the field-effect transistor measurements. All electrical measurements were performed under dry nitrogen atmosphere and under quasi-static conditions with slow scan of source-drain or source-gate voltage. The transfer characteristics for the field-effect transistors (FETs) were measured with the gate voltage (V_G) sweep rate 40 mV/s. The electron mobility was calculated from the slope

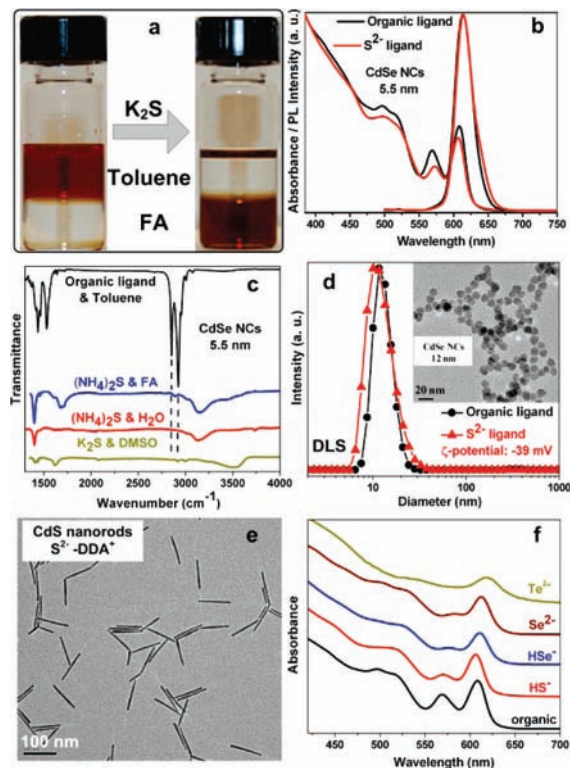


Figure 1. (a) Red colored colloidal dispersion of CdSe NCs undergoes the phase transfer from toluene to formamide (FA) upon exchange of the original organic surface ligands with S²⁻. (b) Absorption and PL spectra of 5.5 nm CdSe NCs capped with organic ligands and S²⁻ ligands dispersed in toluene and FA, respectively. (c) FTIR spectra of 5.5 nm CdSe NCs with different combinations of ligands and solvents. (d) NC size-distributions measured by Dynamic Light Scattering for ~12 nm CdSe NCs capped with organic ligands and S²⁻ ions. Inset shows TEM image of the NCs capped with S²⁻ ligand. (e) TEM images of S²⁻-DDA⁺-capped CdS nanorods. (f) Absorption spectra of 5.5 nm CdSe NCs capped with different ligands.

of the drain current (I_D) versus V_G measured when the gate voltage was scanned in the forward direction (i.e., from negative to positive). For an n-type FET, this measurement typically provides a conservative estimate for the field effect mobility.⁸ Additional details on the mobility calculations provided in the Supporting Information.

3. RESULTS AND DISCUSSION

The NCs used in this work were synthesized following accepted protocols^{14–26} using ligands with long (C₁₂–C₁₈) hydrocarbon tails to control NC size and shape. We did not notice substantial differences in the behavior of NCs capped with the carboxylate, amine, and phosphonate based organic ligands. For a typical ligands exchange procedure, we combined solutions of organics-capped NCs in a nonpolar solvent (toluene or hexane) with the solution of inorganic ligands (K₂S, KHS, (NH₄)₂TeS₃, KOH, KNH₂, etc.) in formamide (FA). The two-phase mixture containing immiscible layers of FA and nonpolar solvent mixture stirred for about 10 min, after which we observed complete transfer of NCs from nonpolar solvent to FA (Figure 1a). Such exchange could be carried out in different solvents, ruling out special role of FA in colloidal stabilization. For example, S²⁻-capped CdSe NCs could be easily prepared using (NH₄)₂S in aqueous medium or Na₂S and K₂S in dimethylsulfoxide (DMSO). However, we could not obtain

colloidal dispersions of S^{2-} -capped NCs in dimethylformamide (DMF) that was chemically similar to FA. Our experimental data showed that colloidal stability of NC dispersions is mainly determined by the solvent dielectric constant; highly polar FA ($\epsilon = 106$) was found to be the best solvent, while water ($\epsilon = 80$) and DMSO ($\epsilon = 47$) provided moderate stability. DMF, the least polar in this series ($\epsilon = 36$), did not stabilize the colloidal dispersions. Below, we summarize and discuss the results obtained for different classes of metal-free inorganic ligands.

3.1. Chalcogenide and Hydrochalcogenide Ligands (S^{2-} , HS^- , Se^{2-} , HSe^- , Te^{2-} , and HTe^-). Figure 1b compares the absorption and PL spectra of 5.5 nm CdSe NCs capped with organic ligands in hexane and S^{2-} in FA. The excitonic features in the absorption spectrum of CdSe NCs remained unchanged after the ligands exchange, implying no changes in size, shape, and size-distribution of CdSe NCs. The NCs with organic ligands showed $\sim 13\%$ PL quantum efficiency (QE) which dropped to about 2% QE for S^{2-} -capped CdSe NCs in FA. The observation of band edge PL from S^{2-} -capped CdSe NCs was rather unexpected since alkylthiols are well-known PL quenchers for CdSe NCs.³¹ It was found that, in contrast to thiols, S^{2-} ligands do not introduce midgap states serving as fast nonradiative recombination channels. CdSe NCs capped with HS^- ligands also retained their band-edge PL (Supporting Information Figure S1). S^{2-} can replace different kinds of organic ligands such as carboxylates, amines, phosphonic acids, and alkylphosphonic oxide from surface of CdSe NCs.

Figure 1c shows FTIR spectra of 5.5 nm CdSe NCs taken before and after the exchange of organic ligands with S^{2-} . The transfer of NCs from toluene to FA resulted in complete disappearance of the bands at 2852 and 2925 cm^{-1} corresponding to C–H stretching in the original organic ligands. Other bands in the FTIR spectra for S^{2-} -capped NCs could be assigned to the solvent and $(NH_4)_2S$ (Figure S2). For example, FTIR spectra of S^{2-} -capped CdSe NCs prepared from water dispersion showed no observable C–H bands. These results confirm the efficacy of S^{2-} ligands in complete removal of the original organic ligands, forming all-inorganic colloidal NCs.

NC surface has numerous electrophilic sites, for example, the surface of CdSe NCs is rich with undercoordinated Cd^{2+} sites. These sites should favor adsorption of nucleophilic S^{2-} ions rather than positively charged counterions (e.g., K^+ or NH_4^+). In addition, in polar solvents, cations are typically more solvated than anions.¹³ The ligands exchange can be described as a nucleophilic substitution at the metal site. Because of sterical crowding around the reaction center, one can expect the dissociative reaction pathway, although detailed kinetic studies would be required to clarify the mechanism of ligands exchange.

Colloidal stabilization of NCs in FA was achieved through binding negatively charged S^{2-} ions to NC surface, leading to the formation of an electrical double layer around each NC. The negative charging of CdSe NC surface resulted in a negative (-40 mV) ζ -potential, sufficient for electrostatic stabilization of the colloidal dispersion. Dynamic light scattering (DLS) studies also confirmed single-particle populations in the solutions of S^{2-} -capped CdSe NCs (Figure 1d, for NCs with the TEM image shown in the inset). The direct comparison of the volume distribution curves calculated from DLS revealed that average hydrodynamic diameter of S^{2-} -capped NCs was smaller by ~ 1.7 nm than that of the same NCs capped with *n*-tetradecylphosphonic acid, which accounted for the effective length of the hydrocarbon chains.

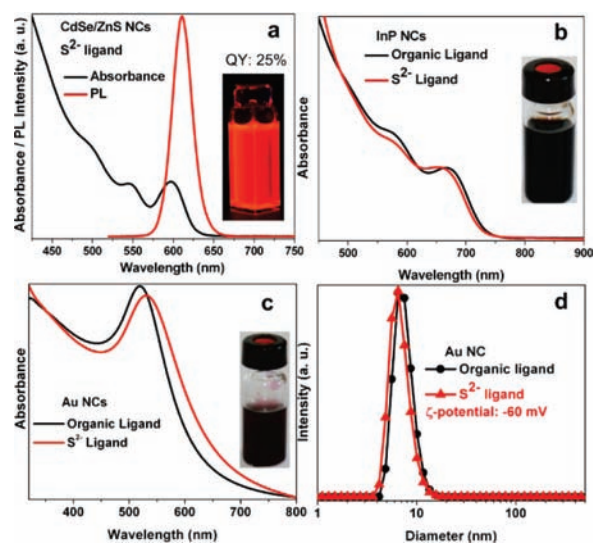


Figure 2. (a) Absorption and PL spectra of CdSe/ZnS core/shell NCs capped with S^{2-} ligands dispersed in FA; inset shows the luminescence of NC dispersion upon illumination with 365 nm UV light. (b) Absorption spectra of InP NCs capped with organic ligands and S^{2-} ligands dispersed in toluene and FA, respectively. Inset shows the optical photograph of colloidal dispersion of InP NCs in FA. (c) Absorption spectra of Au NCs capped with dodecanethiol and S^{2-} ligands dispersed in toluene and FA, respectively. Inset shows the optical photograph of a colloidal dispersion of Au NCs in FA. (d) DLS size-distribution plots for Au NCs capped with the organic and S^{2-} ligands.

In polar solvents like FA, we used small inorganic cations K^+ , Na^+ , NH_4^+ to balance the negative charge of anions adsorbed on the NC surface. These cations could be replaced with hydrophobic quaternary ammonium ions by treatment with didodecyldimethylammonium bromide (DDA^+Br^-), rendering NC insoluble in FA, but soluble in toluene.³² We applied this technique to S^{2-} -capped CdS nanorods. Figure 1e shows a TEM image of S^{2-} - DDA^+ -capped CdS nanorods. The shape and dimensions of nanorods remained intact during the transfer from toluene (ODPA-TOPO ligands) to FA (S^{2-} ligands) to toluene (S^{2-} - DDA^+ ion pair ligands).

Stable colloidal solutions of CdSe NCs could be prepared in FA using different chalcogenide (S^{2-} , Se^{2-} , and Te^{2-}) and hydrochalcogenide (HS^- , HSe^- , and HTe^-) ions. Figure 1f shows the absorption spectra for colloidal solutions of the same CdSe NCs stabilized with different ligands. In all cases of chalcogenide and hydrochalcogenide ligands, we observed the formation of stable colloidal solutions of negatively charged NCs. It should be noted that selenide and telluride ions can be easily oxidized in air and corresponding colloidal solutions should be handled under inert atmosphere.

Chalcogenide ions can stabilize different nanomaterials in polar solvents. For example, Figure 2a shows S^{2-} -capped CdSe/ZnS core-shell NCs with a strong band edge PL with QE about 25%. All-inorganic films of S^{2-} -capped CdSe/ZnS NCs also showed bright emission, even after annealing at 250 $^\circ C$ for 30 min. S^{2-} ligands worked well for InP NCs (Figure 2b) providing the first example of all-inorganic colloidal III–V NCs. The absorption spectra of S^{2-} -capped InP NCs in FA were similar to those of the organically capped NCs in toluene. The ζ -potential of S^{2-} -capped InP NCs was about -60 mV. The ability of chalcogenide ions to provide colloidal stabilization was not

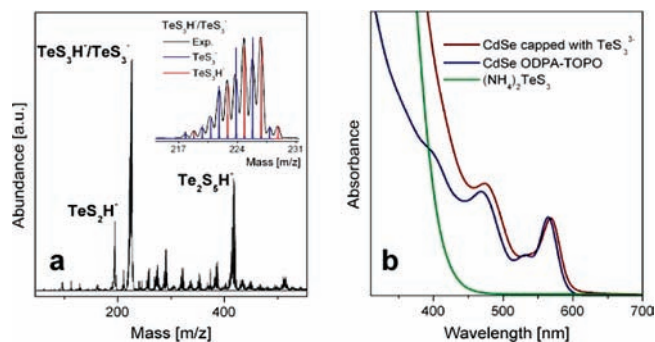


Figure 3. (a) ESI-MS spectrum of $(\text{NH}_4)_2\text{TeS}_3$ solution. The inset compares an experimental high-resolution mass-spectrum with simulated spectra for TeS_3H^- and TeS_3^- ions. (b) Absorption spectra for $(\text{NH}_4)_2\text{TeS}_3$, for CdSe NCs capped with the organic ligands in toluene and for CdSe NCs capped with TeS_3^{2-} ions in formamide.

limited to semiconductors; Figure 2c compares the absorption spectra for spherical 7 nm Au NCs capped with dodecanethiol in toluene and with S^{2-} ions in FA. We observed an 11 nm red-shift for surface plasmon band in S^{2-} -capped Au NCs, consistent with the difference in dielectric constants of toluene and FA.¹⁰ DLS studies revealed that S^{2-} -capped Au colloids retained size distribution after the ligands exchange (Figure 2d), with no agglomeration for both organic and S^{2-} -capped NCs. The ζ -potential of S^{2-} -capped Au NCs was about -60 mV.

Mild oxidation of chalcogenide ions typically results in the formation of polychalcogenide ions (S_n^{2-} , Se_n^{2-} , Te_n^{2-}). In fact, polychalcogenides are often present as an impurity in commercial metal chalcogenide chemicals. As a simple test, aqueous sulfide solutions should be colorless whereas polysulfides absorb visible light and appear yellow to red. We used ESI-MS to identify the presence and stability of polychalcogenides in different solvents. The mass spectra of the red Na_2S_n solution prepared by adding an excess of sulfur to aqueous 0.7 M Na_2S solution showed the presence of polysulfides with $n = 5, 6,$ and 7 unlike to colorless Na_2S solution (Figures S3–S5). We found that both $(\text{NH}_4)_2\text{S}_n$ and Na_2S_n solutions could stabilize colloidal NCs in polar solvents, suggesting that polysulfides behave similarly to sulfide ions. Survey of many samples led us to the conclusion that polysulfides were weaker ligands than S^{2-} . We also could not rule out the possibility of NC passivation with sulfide ions that always coexist in equilibrium with polysulfides in $(\text{NH}_4)_2\text{S}_n$ and Na_2S_n solutions.

3.2. Mixed Chalcogenide TeS_3^{2-} Ligands. Having molecular structure intermediate between MCCs and polychalcogenide ions, mixed chalcogenide ions such as TeS_3^{2-} represent another interesting choice of metal-free ligands. For the proof-of-principle study, we used light-yellow aqueous $(\text{NH}_4)_2\text{TeS}_3$ ²⁹ to stabilize colloidal CdSe NCs via ligand exchange in FA. ESI-MS spectra show that $(\text{NH}_4)_2\text{TeS}_3$ aqueous solution contains mainly TeS_3^{2-} ions along with $\text{Te}_2\text{S}_5^{2-}$ (Figure 3a). Adsorption of submonolayer amounts of $\text{Te}-\text{S}$ ions onto the surface of 4.4 nm CdSe NCs was confirmed by elemental analysis, indicating Te-to-Cd atomic ratio of 0.25. The atomic ratio of S-to-Te equal to 3.67 suggests the adsorption of TeS_3^{2-} ions, along with possibility for some additional S^{2-} incorporating onto the NC surface. Note that Cd-to-Se ratio of 1.25 was similar to that of original NCs. The integrity of CdSe NC core was also evident from the similar excitonic absorption features in the optical absorption spectra (Figure 3b). The main difference lies in the

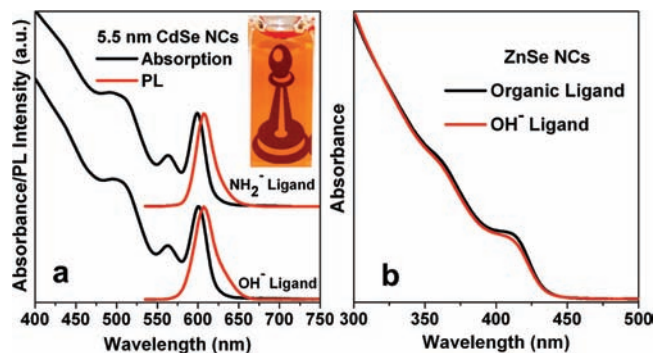


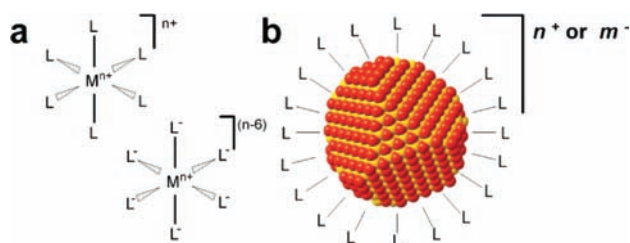
Figure 4. (a) Absorption and PL spectra of OH^- and NH_2^- -capped CdSe NCs dispersed in FA. Inset shows a photograph of the colloidal solution. (b) Absorption spectra of ZnSe NCs capped with oleylamine and OH^- ligands dispersed in toluene and FA, respectively.

high energy part of absorption spectra (≤ 450 nm) showing the contribution from the TeS_3^{2-} ions. Surface affinity of TeS_3^{2-} ions is rather similar to that of MCC ligands. For example, stable colloidal solutions of PbS NCs could be formed with TeS_3^{2-} ions in FA, whereas capping with S^{2-} could not provide stable colloidal solutions for IV–VI NCs.

The presence of two chalcogens in different oxidation states opens interesting possibilities for surface redox reactions. Te^{4+} can oxidize its own ligand (S^{2-}) releasing elemental Te and S, which explains limited stability of $(\text{NH}_4)_2\text{TeS}_3$ in the solid state, under light or heat. Another redox pathway is the reaction of Te^{4+} with the NC material. For example, metal telluride NCs such as CdTe and PbTe slowly reacted with TeS_3^{2-} releasing elemental Te ($\text{Te}^{4+} + \text{Te}^{2-} \rightarrow \text{Te}^0$ comproportionation reaction) and leading to partial or complete conversion to CdS and PbS, respectively. For PbTe NCs, this reaction occurred within minutes after the ligand exchange, while CdTe converted to CdS only upon heating of NC films at 120°C . CdSe NCs are significantly more stable, and only partially react under the thermal treatment (Figure S6). At the same time, PbS NCs do not react with TeS_3^{2-} as confirmed by powder XRD patterns for dried and annealed samples (Figure S7). Therefore, the use of mixed chalcogenide ligands can be advantageous for compositional modulations in nanogranular solid materials such as thermoelectric Pb and Sb chalcogenides.³³

3.3. Other Metal-Free Anionic Ligands (OH^- and NH_2^-). We also explored stabilization of colloidal NCs with other inorganic anions. OH^- and NH_2^- successfully replaced organic ligands at the surface of CdSe NCs and stabilized colloidal solutions in FA. Figure 4a shows that absorption and PL spectra of OH^- and NH_2^- -capped 5.5 nm CdSe NCs did not change compared to original NCs (Figure 1b); no change was also detected in XRD patterns of corresponding NCs (Figure S8). Similar to S^{2-} -capped NCs, OH^- -capped CdSe NCs exhibited negative ζ -potentials in polar solvents, consistent with the electrostatic stabilization. The value of ζ -potential for OH^- -capped CdSe NCs in FA (-20 mV) was substantially lower than that for S^{2-} -capped NCs. Right after the ligand exchange, colloidal solutions could be easily filtered through a $0.2\ \mu\text{m}$ filter but they slowly aggregated and precipitated in several days. Unlike S^{2-} -capped NCs, FTIR spectra of OH^- -capped CdSe NCs (Figure S9) did not show complete removal of CH_2 bands at 2852 and $2925\ \text{cm}^{-1}$, but the intensity of C–H bands decreased by $>90\%$ compared to the original NCs. Similar

Scheme 1. (a) Typical Metal Complexes and (b) a Nano-crystal with Surface Ligands^a



^aWe want to emphasize similarities between metal-ligand (M-L) bonding in both classes of compounds. The HSAB principle, originally developed for metal complexes, should also apply to colloidal nanomaterials.

behavior and ζ -potentials have been observed for NH_2^- -capped CdSe NCs. These observations point to somewhat lower affinity of OH^- and NH_2^- toward CdSe surface compared to chalcogenides. In contrast, ZnSe NCs did not form stable colloidal solutions with S^{2-} ligands but could be easily stabilized with OH^- in FA (Figure 4b). The possible origin of such selectivity will be discussed in the next section.

3.4. Can the Hard and Soft Acids and Bases (HSAB) Classification Be Applied to Colloidal Nanostructures? In 1963 Pearson proposed the HSAB principle that explained many trends in stability of the complexes between Lewis acids and bases by classifying them into “hard” and “soft” categories.³⁴ Generally, soft acids form stable complexes with soft bases, whereas hard acids prefer hard bases. The inorganic ligands used in our work represent classical examples of soft (highly polarizable HS^- , S^{2-} , Se^{2-}) and hard (less polarizable OH^- , NH_2^-) Lewis bases. We noticed that original ligands on Au and CdTe NCs could be easily replaced with S^{2-} , Se^{2-} , or HS^- ligands, but did not form stable colloidal solutions in the presence of OH^- . In contrast, ZnSe (Figure 4b) and ZnO NCs could be stabilized with OH^- but did not interact with S^{2-} and HS^- . Other NCs, including CdSe and CdS, formed stable colloidal solutions with both hard and soft ligands. We attributed this difference in behavior to the differences in chemical affinity between NCs and Lewis bases and proposed that HSAB principle, originally developed for molecular coordination compounds, could be extended to the world of nanomaterials (Scheme 1). The ligands used in our work bind primarily to the electrophilic sites at NC surface. In agreement with HSAB, soft Au^0 and Cd^{2+} sites exhibited stronger affinity to soft S^{2-} and HS^- ligands compared to hard OH^- , whereas harder Zn^{2+} sites in ZnSe and ZnO NCs had higher affinity to OH^- rather than to HS^- . More quantitative information on the binding affinity could be obtained from the comparison of ζ -potentials related to the charges on NC surface (Table S1). The extension of HSAB principle to NCs appears to fail for InP and InAs NCs. Free In^{3+} is a hard acid, while InAs and InP behave as soft acids preferentially binding to S^{2-} and HS^- rather than to OH^- . This discrepancy, however, could be explained by taking into account the character of chemical bonding inside NCs. Small difference in electronegativity between In and P or As led to reduced positive effective charge on the In surface sites, much smaller than the charge on isolated In^{3+} ions. Low charge density softens the acidic sites at InP and InAs NCs surface. To further test this hypothesis, we synthesized In_2O_3 NCs,²⁴ where the bonding has a higher ionic character compared to InP and InAs, and studied their

interaction with OH^- and HS^- ligands. Both HS^- and OH^- bound to In_2O_3 NC surface resulting in similar ζ -potentials (-40 mV), suggesting that the metal surface sites in In_2O_3 NCs were harder than those in InP and InAs NCs. One should understand that the HSAB principle has a limited predictive power and does not necessarily dictate all possible ligand exchange pathways. However, we found HSAB-based generalization of ligand exchange reactions very useful for predicting the binding affinity between a given ligand and a given NC.

3.5. Comparison of Metal-Free Inorganic Ligands to MCCs. Negatively charged metal-free ligands can be viewed as an addition to the family of all-inorganic colloidal NCs that started with the discovery of MCC ligands.^{9,10} In this section, we summarize our observations comparing metal-free inorganic ligands to MCCs.

The solutions of MCCs in polar solvent are expected to contain a certain equilibrium concentration of free chalcogenide ions. We explored the possibility of using chalcogenide ions to prepare stable colloidal solutions of NCs in hydrazine, often used with MCC ligands. It was found that chalcogenides could not stabilize II–VI, IV–VI, and III–V NCs in hydrazine. Probably, the dielectric constant of hydrazine ($\epsilon = 51$) and its solvation ability were not sufficient to obtain stable NC colloids with chalcogenide ligands. In contrast, $\text{Sn}_2\text{Se}_6^{4-}$ and other MCC ligands provided long-term, up to several years, stability to CdSe NC colloids in hydrazine. In FA, both chalcogenides and MCCs generated stable colloidal solutions, for example, for Au and CdSe NCs. Direct comparison revealed that CdSe NCs capped with SnS_4^{4-} or AsS_3^{3-} MCC ligands exhibited higher ζ -potentials, typically in the range of -50 to -80 mV. That probably corresponded to a higher affinity of MCCs toward CdSe NCs. On the other hand, S^{2-} was superior for CdSe/ZnS NCs, for which many MCCs showed poor affinity. MCCs and mixed chalcogenide ligands were better for Pb chalcogenide NCs, for which S^{2-} capping failed. Compared to the MCCs, free chalcogenide ions were somewhat more prone to oxidative degradation. Both, sulfide-based MCC-capped NCs and S^{2-} -capped nanomaterials can be prepared and handled in air, but S^{2-} -capped NCs were much longer stable if prepared and stored in a glovebox (many months).

3.6. Electrostatic Stabilization of Colloidal Nanocrystals in the Absence of Charged Ligands (“Ligand-Free” Nanocrystals). So far we discussed inorganic ligands that provided negative charge to the NCs. All-inorganic positively charged NCs are rarer, presumably because NCs typically have electrophilic metal-rich surfaces with preferential affinity toward nucleophilic ligands. Recently, Murray and co-workers reported colloidal NCs with positively charged surface.³⁵ They used nitrosonium tetrafluoroborate (NOBF_4) and aryldiazonium tetrafluoroborate to perform ligand exchange on Fe_3O_4 , FePt , Bi_2S_3 , and NaYF_4 NCs, resulting in positively charged NC surface. Unfortunately, this approach did not work with CdSe and other semiconductor NCs.³⁵ Nitrosonium salts are known as strong one-electron oxidants,³⁶ resulting in the etching of NC surface immediately after the addition of NOBF_4 (Figure S10).

To cleave the bonds between CdSe NC and carboxylate organic ligands without oxidizing the NCs, we used HBF_4 and HPF_6 in polar solvents. This reaction resulted in the phase transfer of NCs from nonpolar solvent (toluene) to a polar solvent (FA). In the case of oleylamine and oleate capping ligands, H^+ cleaved the Cd–N and Cd–O bonds, as schematically shown in Figure 5a, leaving behind positively charged

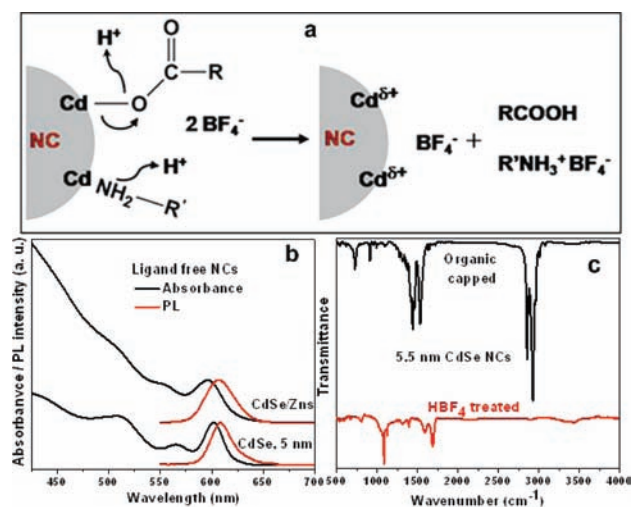


Figure 5. (a) Removal of the organic ligands from the surface of CdSe NCs by HBF_4 treatment. For simplicity, we showed monodentate binding mode of carboxylate group. Proposed mechanism should hold for other chelating and bridging modes as well. (b) Absorption and PL spectra of ligand-free colloidal CdSe and CdSe/ZnS NCs obtained after HBF_4 treatment. (c) FTIR spectra of organically capped and ligand-free CdSe NCs after HBF_4 treatment.

metal sites at the NC surface. HBF_4 treatment was efficient for NCs capped with carboxylate and alkylamine ligands whereas CdSe NCs capped with alkylphosphonic acid remained in the toluene phase even after extended HBF_4 treatment. BF_4^- and PF_6^- are known as very weak nucleophiles.³⁷ These weakly coordinating anions did not bind to the NC surface, instead they acted as counterions in the electrical double layer around NCs. Figure 5b shows the absorption and PL spectra of 5.5 nm CdSe NCs and CdSe/ZnS core–shells after treatment with HBF_4 in FA. The size, size-distribution, and band-edge emission remained, however, with a significant drop in the PL efficiency ($<0.5\%$ for CdSe NCs and $\sim 2\%$ for CdSe/ZnS NCs). ζ -potentials of CdSe and CdSe/ZnS NCs in FA were measured to be around $+30$ mV. Similar values were obtained with HPF_6 . The removal of organic ligands was not possible with NaBF_4 and NaPF_6 , emphasizing the role of H^+ ions in the reaction, which was also suggested in previous reports.³⁵ Figure 5c compares FTIR spectra of CdSe NCs capped with organic ligands and FTIR spectra of the same CdSe NCs after HBF_4 treatment. The absence of C–H bands at 2852 and 2925 cm^{-1} constituted complete removal of the original organic ligand. The band centered at 2890 cm^{-1} was from FA (Figure S2). Apart from the FA related bands, we observed a new sharp band at 1083 cm^{-1} corresponding to BF_4^- ions.

3.7. Colloidal NCs with Metal-Free Inorganic Ligands for Device Applications. The exchange of bulky organic surfactants with small inorganic ligands like S^{2-} or Se^{2-} should substantially facilitate the electronic communication between individual NCs. Indeed, when S^{2-} -capped CdSe NCs were placed next to each other in form of a close-packed film, we observed a red shift of the excitonic peaks in the absorption spectra compared to those for individual NCs dispersed in FA (Figure S11). Such red shift can come from slight relaxation of the quantum confinement due to partial leakage of the wave function into neighboring NCs. The same CdSe NCs capped with the organic ligands showed almost identical absorption spectra in solutions and in close-packed

films. Strong electronic coupling provides an exciting opportunity for the integration of colloidal NCs into electronic and optoelectronic devices. Detailed investigations of the electronic properties of NCs with these new capping ligands will be a subject of a separate study. Here, we show our preliminary results on the electron transport in the arrays of S^{2-} -capped CdSe NCs as well as CdSe/CdS and CdSe/ZnS core–shell NCs.

The electron mobility in NC arrays can be conveniently measured from transfer characteristics of a field-effect transistor.^{6,8} For these studies, 20–40 nm thick close packed NC films were deposited on highly doped Si wafers with 100 nm thick SiO_2 thermal gate oxide. The NC films were spin-coated from FA solutions at elevated temperatures (80 °C), followed by short annealing at 200 – 250 °C. Source and drain Al electrodes were patterned on the annealed NC films using a shadow mask. Figure 6a–c shows sets of drain current (I_D) versus drain-source voltage (V_{DS}) scans at different gate voltages (V_G) for devices made of $(\text{NH}_4)_2\text{S}$ -capped 4.6 nm CdSe NCs (originally capped with oleylamine and oleic acid), 10 nm CdSe/CdS, and 8 nm CdSe/ZnS core/shell NCs. I_D increased with increasing V_G , characteristic of the n-type transport. Both transfer and output characteristics of our FETs were generally reproducible during multiple voltage scans.

The electron mobility corresponding to the linear regime of FET operation (measured at $V_{DS} = 2$ V across a 80 μm long channel) for a film of CdSe NCs capped with $(\text{NH}_4)_2\text{S}$ annealed at 200 °C was $\mu_{\text{lin}} = 0.4$ $\text{cm}^2 \text{V}^{-1} \text{s}^{-1}$ with $I_{\text{ON}}/I_{\text{OFF}} \sim 10^3$ (Figure 6a,d). FETs assembled from CdSe/CdS (Figure 6b,e) and CdSe/ZnS (Figure 6c,f) core–shell NCs capped with $(\text{NH}_4)_2\text{S}$ ligands annealed at 250 °C showed $\mu_{\text{lin}} = 0.04$ $\text{cm}^2 \text{V}^{-1} \text{s}^{-1}$ with $I_{\text{ON}}/I_{\text{OFF}} \sim 10^4$ at $V_{DS} = 2$ V and $\mu_{\text{lin}} = 6 \times 10^{-5}$ $\text{cm}^2 \text{V}^{-1} \text{s}^{-1}$ with $I_{\text{ON}}/I_{\text{OFF}} \sim 10^2$ at $V_{DS} = 4$ V, respectively. The electron mobility measured in the saturation mode of FET operation ($V_{DS} = 30$ V, Figure S12) was slightly higher than μ_{lin} for CdSe and CdSe/ZnS NCs: 0.5 and 9×10^{-5} $\text{cm}^2 \text{V}^{-1} \text{s}^{-1}$, respectively. The devices assembled from CdSe/CdS core–shell NCs showed similar electron mobility in both linear and saturation regimes. Measured electron mobility depends both on the intrinsic property of the material, and on a number of parameters related to device characteristics (FET structure, gate dielectric, film uniformity, contacts, etc.). There are all reasons to expect that higher mobility will be obtained after further optimization of FET devices.

The channel currents were orders of magnitude lower for CdSe NCs capped with K_2S ligands as compared to $(\text{NH}_4)_2\text{S}$ ligands. We attributed low conductivity to the presence of K^+ ions creating local electrostatic barriers around NCs and behaving as the electron scattering centers. In contrast, when we used $(\text{NH}_4)_2\text{S}$ to stabilize the solution of CdSe NCs, the mild thermal treatment resulted in the removal of residual solvent and surface ligands and led to much higher carrier mobility in the NC array. The devices assembled from CdSe NCs capped with $(\text{NH}_4)_2\text{TeS}_3$ also showed n-type transport with $\mu_{\text{lin}} = 0.01$ $\text{cm}^2 \text{V}^{-1} \text{s}^{-1}$ (Figure S13).

Although the films of CdSe/ZnS core–shell NCs showed rather low carrier mobility, these NCs preserved bright band-edge photoluminescence even after annealing at 250 °C (insets in Figure 6c). Generally, metal-free ligands allowed obtaining conductive NC layers without introducing foreign metal ions that often introduce recombination centers. As a result, we were able to observe for the first time efficient band-edge PL in electronically conductive NC arrays (Figure 6c).

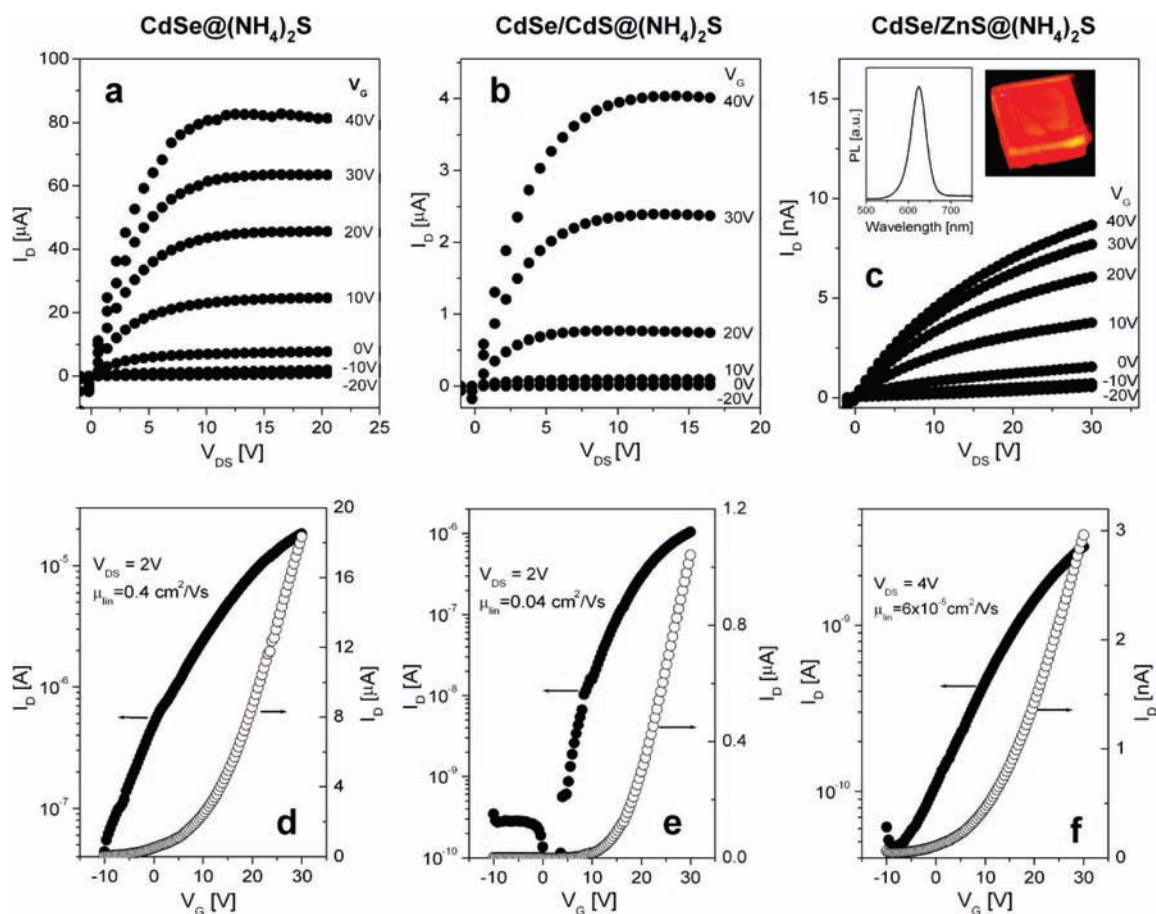


Figure 6. (a–c) Plots of drain current I_D vs drain-source voltage V_{DS} , measured at different gate voltages V_G for the field-effect transistors (FETs) assembled from colloidal NCs capped with $(\text{NH}_4)_2\text{S}$: (a) CdSe, (b) CdSe/CdS core–shells and (c) CdSe/ZnS core–shells. Insets to panel (c) show the photoluminescence spectrum (left) and a photograph (right) for CdSe/ZnS NC film capped with $(\text{NH}_4)_2\text{S}$ ligands annealed at 250 °C for 30 min. (d and e) Plots of I_D vs V_G at constant $V_{DS} = 2 \text{ V}$ used to calculate current modulation and linear regime field-effect mobility for FETs using CdSe and CdSe/CdS NCs. (f) Plots of I_D vs V_G measured at constant $V_{DS} = 4 \text{ V}$ in a FET assembled from CdSe/ZnS NCs. $L = 80 \mu\text{m}$, $W = 1500 \mu\text{m}$, 100 nm SiO_2 gate oxide.

4. CONCLUSIONS

We have demonstrated that various metal-free inorganic ligands like S^{2-} , OH^- , and NH_2^- can behave as capping ligands for colloidal semiconductor and metallic NCs. These ligands significantly enrich the colloidal chemistry of all-inorganic NCs, and represent a promising strategy for integration of colloidal nanostructures in electronic and optoelectronic devices.

■ ASSOCIATED CONTENT

Supporting Information. Additional experimental details, figures and tables. This material is available free of charge via the Internet at <http://pubs.acs.org>.

■ AUTHOR INFORMATION

Corresponding Author
dvtalpin@uchicago.edu

■ ACKNOWLEDGMENT

We thank C. Jiang, M. Bodnarchuk, S. Rupich and J. Huang for help with NC synthesis. We also thank the Analytical Chemistry

Laboratory at Argonne National Lab (ANL) for ICP-OES elemental analysis and Evident Technologies, Inc. for providing samples of high-quality CdSe and CdSe/ZnS NCs. The work was supported by NSF CAREER under Award Number DMR-0847535 and by NSF SBIR Award Number IIP-1047180. D.V.T. thanks the David and Lucile Packard Foundation for their generous support. The work at the Center for Nanoscale Materials (ANL) was supported by the US Department of Energy under Contract No. DE-AC02-06CH11357.

■ REFERENCES

- (1) Coe, S.; Woo, W. K.; Bawendi, M.; Bulovic, V. *Nature* **2002**, *420*, 800–803.
- (2) Gur, I.; Fromer, N. A.; Geier, M. L.; Alivisatos, A. P. *Science* **2005**, *310*, 462–465.
- (3) Konstantatos, G.; Howard, I.; Fischer, A.; Hoogland, S.; Clifford, J.; Klem, E.; Levina, L.; Sargent, E. H. *Nature* **2006**, *442*, 180–183.
- (4) Nag, A.; Kumar, A.; Kiran, P. P.; Chakraborty, S.; Kumar, G. R.; Sarma, D. D. *J. Phys. Chem. C* **2008**, *112*, 8229–8233.
- (5) Yu, D.; Wang, C. J.; Guyot-Sionnest, P. *Science* **2003**, *300*, 1277–1280.
- (6) Talpin, D. V.; Murray, C. B. *Science* **2005**, *310*, 86–89.
- (7) Law, M.; Luther, J. M.; Song, O.; Hughes, B. K.; Perkins, C. L.; Nozik, A. J. *J. Am. Chem. Soc.* **2008**, *130*, 5974–5985.

- (8) Talapin, D. V.; Lee, J. S.; Kovalenko, M. V.; Shevchenko, E. V. *Chem. Rev.* **2010**, *110*, 389–458.
- (9) Kovalenko, M. V.; Scheele, M.; Talapin, D. V. *Science* **2009**, *324*, 1417–1420.
- (10) Kovalenko, M. V.; Bodnarchuk, M. I.; Zaumseil, J.; Lee, J. S.; Talapin, D. V. *J. Am. Chem. Soc.* **2010**, *132*, 10085–10092.
- (11) Lee, J. S.; Kovalenko, M. V.; Huang, J.; Chung, D. S.; Talapin, D. V. *Nat. Nanotech.* **2011**, *6*, 348–352.
- (12) Linder, E.; Picton, H. J. *Chem. Soc.* **1905**, *87*, 1906–1936.
- (13) Verwey, E. J. W. *Chem. Rev.* **1935**, *16*, 363–415.
- (14) Yang, Y. A.; Wu, H. M.; Williams, K. R.; Cao, Y. C. *Angew. Chem., Int. Ed.* **2005**, *44*, 6712–6715.
- (15) Carbone, L.; Nobile, C.; De Giorgi, M.; Sala, F. D.; Morello, G.; Pompa, P.; Hytch, M.; Snoeck, E.; Fiore, A.; Franchini, I. R.; Nadasan, M.; Silvestre, A. F.; Chiodo, L.; Kudera, S.; Cingolani, R.; Krahn, R.; Manna, L. *Nano Lett.* **2007**, *7*, 2942–2950.
- (16) Talapin, D. V.; Rogach, A. L.; Kornowski, A.; Haase, M.; Weller, H. *Nano Lett.* **2001**, *1*, 207–211.
- (17) Micic, O. I.; Curtis, C. J.; Jones, K. M.; Sprague, J. R.; Nozik, A. J. *J. Phys. Chem.* **1994**, *98*, 4966–4969.
- (18) Talapin, D. V.; Gaponik, N.; Borchert, H.; Rogach, A. L.; Haase, M.; Weller, H. *J. Phys. Chem. B* **2002**, *106*, 12659–12663.
- (19) Guzelian, A. A.; Banin, U.; Kadavanich, A. V.; Peng, X.; Alivisatos, A. P. *Appl. Phys. Lett.* **1996**, *69*, 1432–1434.
- (20) Cao, Y. W.; Banin, U. *J. Am. Chem. Soc.* **2000**, *122*, 9692–9702.
- (21) Zheng, N.; Fan, J.; Stucky, G. D. *J. Am. Chem. Soc.* **2006**, *128*, 6550–6551.
- (22) Cozzoli, P. D.; Manna, L.; Curri, M. L.; Kudera, S.; Giannini, C.; Striccoli, M.; Agostiano, A. *Chem. Mater.* **2005**, *17*, 1296–1306.
- (23) Talapin, D. V.; Nelson, J. H.; Shevchenko, E. V.; Aloni, S.; Sadtler, B.; Alivisatos, A. P. *Nano Lett.* **2007**, *7*, 2951–2959.
- (24) Seo, W. S.; Jo, H. H.; Lee, K.; Park, J. T. *Adv. Mater.* **2003**, *15*, 795–797.
- (25) Yu, W. W.; Wang, Y. A.; Peng, X. G. *Chem. Mater.* **2003**, *15*, 4300–4308.
- (26) Hines, M. A.; Scholes, G. D. *Adv. Mater.* **2003**, *15*, 1844–1849.
- (27) Brauer, G.; *Handbook of Preparative Inorganic Chemistry*; Academic Press, Inc.: New York, 1963.
- (28) Schultz, L. D. *Inorg. Chim. Acta* **1990**, *176*, 271–275.
- (29) Gerl, H.; Eisenman, B.; Roth, P.; Schafer, H. Z. *Anorg. Allg. Chem.* **1974**, *407*, 135–143.
- (30) Pons, T.; Uyeda, H. T.; Medintz, I. L.; Mattoussi, H. *J. Phys. Chem. B* **2006**, *110*, 20308–20316.
- (31) Rogach, A. L.; Kornowski, A.; Gao, M. Y.; Eychmuller, A.; Weller, H. *J. Phys. Chem. B* **1999**, *103*, 3065–3069.
- (32) Kovalenko, M. V.; Bodnarchuk, M. I.; Talapin, D. V. *J. Am. Chem. Soc.* **2010**, *132*, 15124–15126.
- (33) Kovalenko, M. V.; Spokoyny, B.; Lee, J. S.; Scheele, M.; Weber, A.; Perera, S.; Landry, D.; Talapin, D. V. *J. Am. Chem. Soc.* **2010**, *132*, 6686–6695.
- (34) Pearson, R. G. *J. Am. Chem. Soc.* **1963**, *85*, 3533–3569.
- (35) Dong, A. G.; Ye, X. C.; Chen, J.; Kang, Y. J.; Gordon, T.; Kikkawa, J. M.; Murray, C. B. *J. Am. Chem. Soc.* **2010**, *133*, 998–1006.
- (36) Connelly, N. G.; Geiger, W. E. *Chem. Rev.* **1996**, *96*, 877–910.
- (37) Krossing, I.; Raabe, I. *Angew. Chem., Int. Ed.* **2004**, *43*, 2066–2090.